J Appl Electrochem (2008) 38:1329–1337
DOI 10.1007/s10800-008-9563-x

ORIGINAL PAPER

Preparation of a PVA/HAP composite polymer membrane for a direct ethanol fuel cell (DEFC)

Chun-Chen Yang · Ying-Jeng Lee · Shwu-Jer Chiu · Kuo-Tong Lee · Wen-Chen Chien · Che-Tseng Lin · Ching-An Huang

Received: 14 September 2007 / Revised: 7 April 2008 / Accepted: 7 April 2008 / Published online: 19 April 2008

Abstract A novel PVA/Hydroxyapatite (HAP) composite polymer membrane was prepared by the direct blend process and solution casting method. The characteristic properties of the PVA/HAP composite polymer membranes were investigated using thermal gravimetric analysis (TGA), X-ray diffraction (XRD), scanning electron microscopy (SEM), micro-Raman spectroscopy and the AC impedance method. An alkaline direct ethanol fuel cell, consisting of an air cathode with MnO_2 carbon inks based on Ni-foam, an anode with PtRu black on Ni-foam, and the PVA/HAP composite polymer membrane, was assembled and investigated. It was found that the alkaline direct ethanol fuel cell comprising of a novel cheap PVA/HAP composite polymer membrane showed an improved electrochemical performance in ambient temperature and air. As a result, the maximum power density of the alkaline DEFC, using a PtRu anode based on Ni-foam (10.74 mW cm^{-2}), is higher than that of DEFC using an E-TEK PtRu anode based on carbon (7.56 mW cm^{-2}) in an 8M KOH + 2M C_2H_5OH solution at ambient temperature and air. These PVA/HAP composite polymer membranes are a potential candidate for alkaline DEFC applications.

Keywords PVA/HAP · Composite · Polymer membrane · Direct ethanol fuel cell (DEFC) · Alkaline

C.-C. Yang (✉) · Y.-J. Lee · S.-J. Chiu · K.-T. Lee · W.-C. Chien · C.-T. Lin
Department of Chemical Engineering, Mingchi University of Technology, Taipei Hsien 243, Taiwan, R.O.C
e-mail: ccyang@ccsun.mit.edu.tw

C.-A. Huang
Department of Mechanical Engineering, Chang Guang University, Taoyuan 333, Taiwan, R.O.C

1 Introduction

Ethanol is often considered as a renewable liquid fuel for a direct ethanol fuel cell (DEFC). Ethanol is much safer and can be produced in great quantities by fermentation of sugar-containing materials. DEFCs [1–13] have recently received a lot of attention due to their high-energy density and low emission of pollutants. The DEFC has attracted much attention because of its usage of liquid fuel, which simplifies the problems of delivery and storage and its very high theoretical mass energy density (7,440 Wh kg^{-1}). More importantly, liquid fuel can be used at ambient temperature and pressure, which makes the DEFC easy to use with portable 3C electronic devices [1–13].

However, the development of the DEFC has faced several serious problems: (i) slow ethanol oxidation kinetics and incomplete electrooxidation of ethanol (ii) the poisoning of absorbed intermediate species on the Pt surface, (iii) the high ethanol crossover through the polymer membrane, and (iv) the high costs of the Nafion polymer membrane and Pt catalyst.

Presently, the perfluorosulfonate ionomer membranes, such as the Nafion membrane (DuPont), are the primary polymer membranes used on the DEFC. However, the commercial Nafion polymer membranes showed an ethanol crossover problem (facing the same problem as in the methanol crossover), in which ethanol permeates from the anode to the cathode. The ethanol permeation not only causes a loss of fuel but also forms a mixed potential at the cathode and leads to a lower electrochemical performance of the DEFC. Thus, the most important property of the solid polymer membrane on the DEFC is a lower ethanol permeation of a liquid fuel. It is well known that alcohol electrooxidation in alkaline media is much less influenced by the reaction of the intermediate species.

Recently, Verma et al. [14–18] studied alkaline fuel cell systems using methanol, ethanol, and sodium borohydride as fuel. They [15] also prepared the MnO_2 as a cathode catalyst, using it on the flowing alkaline alcohol fuel cell. Yang [19–21] prepared the alkaline crosslinked PVA composite polymer membranes applied on the DMFC. More importantly, the carbonation problem of the alkaline DEFC can be avoided by using alkaline solid polymer membranes instead of an alkaline solution [13]. In addition, as we know, the anodic electrooxidation of alcohol in an alkaline media is much faster than that in an acidic media [22].

Hydroxyapatite ($Ca_{10}(PO_4)_6(OH)_2$, HAP) has long been used as an implant material owing to its excellent biocompatibility, bioactivity and chemical stability. The addition of hydrophilic hydroxyapatite (HAP) ceramic fillers to a polymer matrix not only facilitated a reduction of the glass transition temperature (T_g), the crystallinity of the PVA polymer, and the increase of the amorphous phases of polymer matrix, but also increased its ionic conductivity. There are various ceramic fillers, such as Al_2O_3, TiO_2 [23], SiO_2 [24] and hydroxyapatite (HAP) [25], which have been extensively studied.

Interestingly, Park and Yamazaki [25] recently prepared a Nafion/HAP composite membrane to suppress methanol crossover for a direct methanol fuel cell. They found that the crystallinity of the composite membranes increases with HAP content while the content of water uptake decreases gradually. It was suggested that the higher crystallinity and the lower water uptake of the Nafion/HAP composite membranes resulted in the suppression of methanol crossover.

As we know, when the hydrophilic HAP filler, which is a stiffer material, is added into the PVA matrix, the swelling ratio of the PVA/HAP composite polymer membrane is effectively reduced. Both the dimension stability and the swelling ratio of the composite polymer membranes were improved.

The results indicated that the ionic conductivity and the thermal and dimensional stability properties of the composite polymer membranes were enhanced when a suitable number of the HAP fillers were added into the solid polymer electrolytes (SPEs). As the HAP fillers in the polymer matrix created some defects or amorphous domains or free volumes at the interface between the ceramic particle and the polymer chain, an increase in ionic conductivity of the composite polymer electrolyte occurred. In this composite polymer membrane, there was a dispersion of the HAP fillers into the PVA matrix, which acted as a plasticizer capable of enhancing the chemical and thermal properties and the dimensional stability for the PVA composite polymer membrane.

Up until now, there has been little literature data on the alkaline PVA/HAP composite polymer membrane for the DEFC. In this work, the alkaline DEFC, composing of the air cathode loaded with MnO_2/XC 72R carbon inks, the PtRu black anode based on the Ni-foam (4.00 mg cm^{-2}) and a PVA/HAP composite polymer membrane, was assembled and studied. The PVA/HAP composite polymer membrane was first prepared through a direct blend of the PVA polymer with HAP fillers under an ultrasonic condition. The composite polymer membrane obtained from this process was then further immersed in a 5 wt.% glutaraldehyde (GA) solution for the crosslinking reaction. The anodic ethanol electro-oxidation reaction, the cathodic oxygen reduction reaction (ORR) and the overall reaction of the DEFC in an alkaline media can be described as follows:

Anodic reaction:

$$C_2H_5OH + 12OH^- \rightarrow 2CO_2 + 9H_2O + 12e^-, \quad E_a^0 = -0.743\ \text{V (vs. SHE)}, \tag{1}$$

Cathodic reaction:

$$3O_2 + 6H_2O + 12e^- \rightarrow 12OH^-,\ E_c^0 = 0.401\ \text{V (vs. SHE)}, \tag{2}$$

Overall reaction:

$$C_2H_5OH + 3O_2 \rightarrow 2CO_2 + 3H_2O,\ E_{cell}^0 = 1.143\ \text{V}, \tag{3}$$

The electrochemical characteristics of the DEFC comprising of alkaline PVA/HAP composite polymer membranes were investigated by the linear polarization and the potentiostatic methods; especially, in terms of the peak power density of the DEFC.

2 Experimental

2.1 Preparation of the PVA/HAP composite polymer membrane

PVA (Aldrich), HAP ceramic fillers (Aldrich), and KOH (Merck) were used without further purification. The degree of polymerization and saponification of the PVA were 1,700 and 98 ~ 99%, respectively. The PVA/HAP composite polymer membranes were prepared using a solution casting method. The appropriate weight ratios of the PVA:-HAP = 1:2.5 ~ 10 wt.% were dissolved in distilled water by stirring. The resulting solution was stirred continuously until the solution mixture reached a homogeneous viscous appearance at 90 °C for 2 h. The addition of the sequence of HAP powders and the time of the blend in the vessel were well controlled. The resulting solution was poured out onto a glass plate or Petri dish. The thickness of the wet composite polymer membrane was between 0.20 and 0.40 mm. The

container with the viscous PVA/HAP composite polymer solution was weighed again and then excess water was allowed to evaporate slowly at 25 °C with a relative humidity of 30 RH%. After water evaporation, the container with the composite solid polymer membrane was weighed again. The composition of the PVA/HAP composite polymer membrane was determined from the mass balance. The thickness of the composite polymer membrane was controlled in the range of 0.10–0.30 mm.

The PVA/HAP composite polymer membrane was further crosslinked by immersion in a solution of 5 wt.% glutaraldehyde (GA, 25 wt.% content in distilled water, Merck), 1.0 vol.% HCl (as a catalyst) and acetone for the crosslinking reaction at 40 °C for 12 h. The preparation methods of the PVA composite polymer electrolyte membranes by a solution casting method have been reported in detail elsewhere [19–21].

2.2 Crystal structure, morphology, and thermal analyses

TGA thermal analysis was carried out using a Perkim Elmer Pyris 7 TGA system. Measurements were carried out by heating from 25 °C to 600 °C under N_2 atmosphere at a heating rate of 10 °C min^{-1} with about a 10 mg sample.

The crystalline structures of all the PVA/HAP composite polymer membranes were examined using a Philips X'Pert X-ray diffractometer (XRD) with a Cu Kα radiation of wavelength $\lambda = 1.54056$ Å for 2θ angles between 10 and 90°. The cross-sectional view and top surface morphologies and microstructures of all PVA/HAP composite polymer membranes were investigated by a Hitachi S-2600H scanning electron microscope (SEM).

2.3 Ionic conductivity measurements

Conductivity measurements were made for an alkaline PVA/HAP composite polymer membrane by an AC impedance method. The PVA/HAP composite samples were immersed in an 8M KOH solution for at least 24 h before the test. The alkaline PVA/HAP composite polymer membranes were placed between SS304 stainless steel, ion-blocking electrodes, with a surface area of 1.32 cm^2, in a spring-loaded glass holder. A thermocouple was kept close to the composite polymer membrane for a temperature measurement. Each sample was equilibrated at the experimental temperature for at least 30 min before measurement. AC impedance measurements were carried out using Autolab PGSTAT-30 equipment (Eco Chemie B.V., Netherlands). An AC frequency range of 300 kHz to 100 Hz at an excitation signal of 5 mV was recorded. The impedance of the composite polymer membrane was recorded at a temperature range of 30–70 °C. Experimental temperatures were maintained within ±0.5 °C by a convection oven. All alkaline PVA/HAP composite polymer membranes were examined at least three times.

2.4 Micro-Raman spectroscopy analyses

Micro-Raman spectroscopy was used to characterize the composition of the PVA/HAP composite polymer membrane. The micro-Raman spectroscopy measurements were carried out by a Renishaw confocal microscopy Raman spectroscopy system with a microscope equipped with a 50× objective and a charge coupled device (CCD) detector. The Raman excitation source was provided with a 633 nm He–Ne laser beam, which had a beam power of 25 mW and was focused on the sample with a spot size of about 1 μm in diameter.

2.5 Preparation of the anode and cathode electrodes

The preparation of the catalyst ink for the anode was prepared by mixing 70 wt.% PtRu black inks (Alfa, HiSPEC 6000, PtRu black with Pt:Ru = 1:1 molar ratio), 30 wt.% PTFE binder solution (DuPont, 60 wt.% base solution), and a suitable amount of distilled water and alcohol. The resulting PtRu black mixtures were ultrasonicated for 2 h. The PtRu black inks were loaded onto the Ni-foam matrix by a paint–brush method to achieve a loading of PtRu black of 4.0 mg cm^{-2}. The as-prepared PtRu anode was dried in a vacuum oven at 100 °C for 12 h.

The carbon slurry for the gas diffusion layer of the air cathode was prepared with a mixture of 70 wt.% Shawinigan acetylene black (AB50) with specific surface area of 80 m^2 g^{-1} and 30 wt.% PTFE (30J binder, DuPont) as a wet-proofing agent and binder. The carbon slurry was coated on the Ni-foam as a current collector and then pressed at 120 kg_f cm^{-2}. The gas diffusion layer was then sintered at temperature of 370 °C for 30 min. The catalyst layer of the air electrode was then prepared by spraying a mixture of a 15 wt.% of PTFE solution binder and 85 wt.% of mixed powders consisting of a γ-MnO_2 (electrolytic manganese dioxide) catalyst supported on XC 72R carbon black. The Ni-foam current collector was cut at 1 × 1 cm^2. The preparation method of the air cathodes has been reported in detail elsewhere [20–21].

2.6 Electrochemical measurements

The PVA/HAP composite polymer membrane was placed between the sheets of the anode and the cathode, and then hot-pressed at 60 °C for 120 kg_f cm^{-2} for 3 ∼ 5 min to obtain a membrane electrode assembly (MEA). The electrode area of the MEA was about 1 cm^2.

The electrochemical measurements were carried out in a two-electrode system. The i–t, E–t and the power density curves of the DEFC comprising of an alkaline PVA/HAP composite polymer membrane were recorded at the potential of 0.40 V, at the current density of 20 mA cm^{-2}, respectively. All electrochemical measurements were performed on an Autolab PGSTAT-30 electrochemical system with GPES 4.8 package software (Eco Chemie, The Netherland). The electrochemical performances of the DEFC comprising of a PVA/HAP composite polymer membrane, and the cathode open to atmospheric air, were studied in an 8M KOH + 2M C_2H_5OH solution in ambient temperatures and air. The construction of an alkaline DEFC for test has been described in detail elsewhere [19–21].

3 Results and discussion

3.1 TGA thermal analysis

Figure 1 shows the TGA and differential gravimetric analysis (DTG) thermographs of the PVA/HAP composite polymer membrane with various HAP compositions. TGA and DTG curves of the PVA/HAP polymer films revealed three main weight loss regions, which appeared as three peaks in the DTG curves. The first region, at a temperature of 80 ~ 100°C ($T_{max,1}$ at 100 °C), was due to the evaporation of physically weak and chemically strong bound H_2O; the weight loss of the membrane was about 2.5 ~ 3.7 wt.%. The second transitional region, at around 350 ~ 380 °C ($T_{max,2}$ at 363 °C), appeared due to the degradation of the side-chain of the PVA/HAP polymer membrane; the total weight loss corresponding to this stage was about 38 ~ 46 wt.%. The peak of the third stage at 440 °C ($T_{max,3}$ at 440 °C) occurred due to the cleavage C–C backbone of PVA/HAP polymer membrane, the so-called carbonation, with a total weight loss at about 90 wt.% at 600 °C, as listed in Table 1.

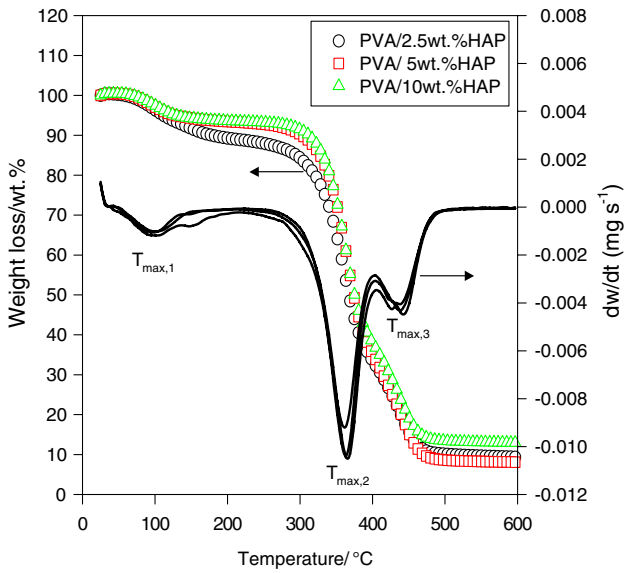

Fig. 1 TGA thermographs of the PVA/HAP composite polymer membranes with different compositions of HAP fillers

Overall, the degradation peaks of the crosslinked PVA/HAP composite polymer samples were less intense and shifted towards higher temperatures. It may therefore be concluded that the improved thermal stability was probably due to the additive effect of the HAP fillers and the chemical crosslink reaction between the PVA and GA.

3.2 Surface morphology, X-ray diffraction and micro-Raman analyses

SEM photographs of the cross-sectional view of the PVA/HAP composite polymer membrane with 5, 10, 15 wt.% HAP fillers are shown in Fig. 2a, b and c, respectively. It was found that PVA/HAP composite membranes with 5% and 10 wt.% HAP fillers were homogenous. However, when the HAP filler content was 15 wt.%, the HAP fillers were to form large aggregates or chucks, as shown in Fig. 2c. In particular, there were some voids in these aggregates, existing at an interface area of flake-like HAP fillers. Figure 2d shows an SEM photograph of the top surface morphology of the PVA/15 wt.%HAP composite membrane, which shows many HAP fillers and large aggregates, and which are randomly distributed on the membrane surface. It was found that the dimension of HAP fillers (with a flake-like structure) deeply embedded in the PVA polymer matrix varied from 50 to 200 μm, as shown in the inset of Fig. 2d. An SEM photograph of the HAP fillers is also shown in the inset of Fig. 2d for comparison.

However, a suitable amount of hydrophilic PVA polymer versus HAP ceramic fillers should be used in order to obtain a uniform and well-dispersed composite polymer membrane. Overall, the compatibility of the PVA polymer and HAP ceramic fillers is good when the HAP content is less than 10 wt.%. As we know, the HAP fillers (which can be used effectively as a ethanol permeation barrier) in the

Table 1 The results of weight loss of the PVA/HAP composite polymer membranes at various temperatures

%	Temperature			
Types	100 °C	250 °C	350 °C	600 °C
HAP powders	0.68	6.81	2.79	3.49
PVA film	0.63	8.00	73.10	92.24
PVA/2.5 wt.%HAP	3.75	12.13	35.98	90.67
PVA/5 wt.%HAP	2.93	7.26	27.96	91.90
PVA/10 wt.%HAP	2.58	6.81	27.39	87.06

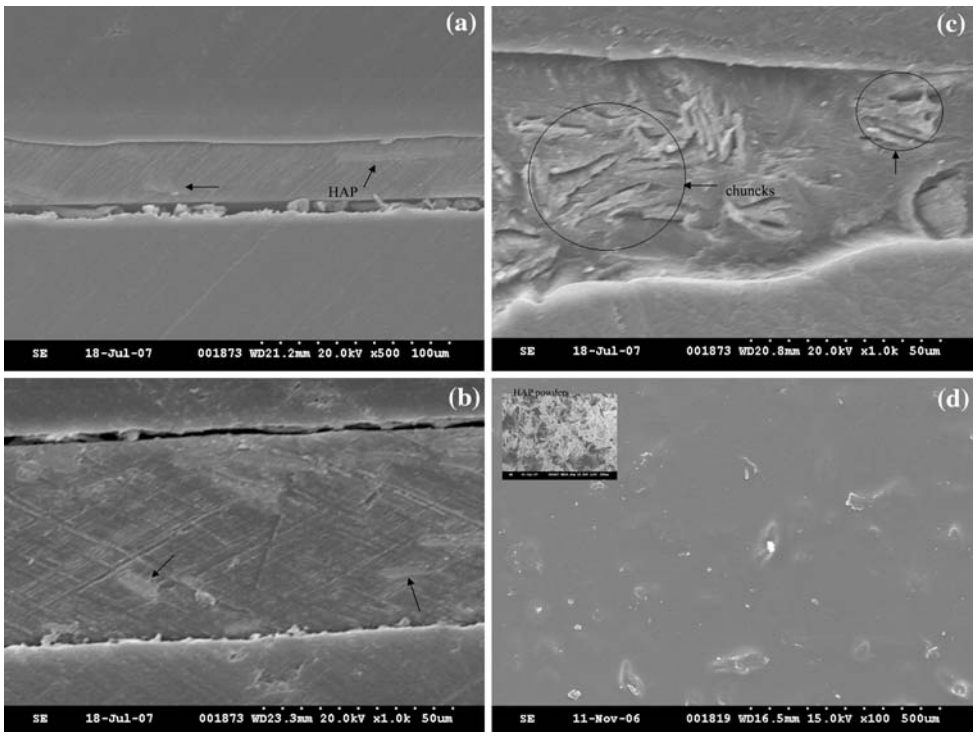

Fig. 2 SEM photographs of the PVA/x wt.%HAP composite polymer membranes; Cross-sectional view: (**a**). 5 wt.%; (**b**). 10 wt.%; (**c**). 15 wt.%; Top view: (**d**). PVA/5 wt.%HAP SPE (top view) and HAP powders (the inset)

PVA matrix can assist in reducing ethanol crossover through the composite polymer membrane.

An X-ray diffraction measurement was performed to examine the crystallinity of the PVA/HAP composite polymer membrane. Figure 3 shows the diffraction pattern of the PVA/HAP composite polymer membranes which were prepared by a blending process with different HAP compositions. It has been well known that the PVA polymer exhibits a semi-crystalline structure with a large peak at a 2θ angle of 19 $\sim$ 20°, and a small peak of 39 $\sim$ 41° [14–17]. As seen in Fig. 3, a large peak at 2θ of 20° for the PVA/2.5 $\sim$ 10 wt.%HAP composite membranes was clear. But, it was clearly seen also that the peak intensity of XRD for the PVA/HAP composite polymer films was reduced when the amount of HAP fillers increased. Under such circumstances, it became clear that the amorphous domains in the PVA/HAP composite polymer membrane had been markedly augmented (i.e. that the degree of crystallinity decreased).

Figure 4a shows the micro-Raman spectra of PVA powders and the PVA polymer membrane, which shows some strong characteristic scattering peaks of the PVA polymer at 1,440, 1,145, 926, 852 cm^{-1}, respectively. Figure 4b shows the micro-Raman spectra of the PVA/HAP composite polymer membranes at different HAP compositions. It can be seen clearly from Raman spectra that the strong characteristic scattering peak of HAP fillers at 958 cm^{-1} was for $-PO_4$, due to the P–O stretching. By comparison, the strong peak of the PVA polymer at 1,438 cm^{-1} was due to the C–H bending and O–H bending. Moreover, the two additional

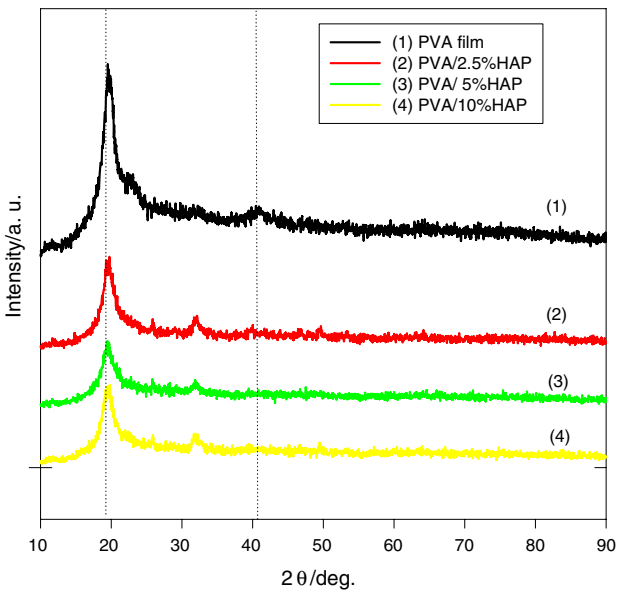

Fig. 3 XRD patterns of the PVA/HAP composite polymer membranes with different HAP compositions

vibrational peaks of the PVA polymer at 912 and 851 cm^{-1} were due to the C–C stretching. Additionally, there were several weak scattering peaks at 1,145 and 1,088 cm^{-1}, which were due to the C–C stretching and C–O stretching, as is also shown in Fig. 4a and listed in Table 2. Most importantly, it can be seen clearly that the intensities of those characteristic vibrational peaks of these PVA/HAP composite polymer membranes had decreased; in particular, a

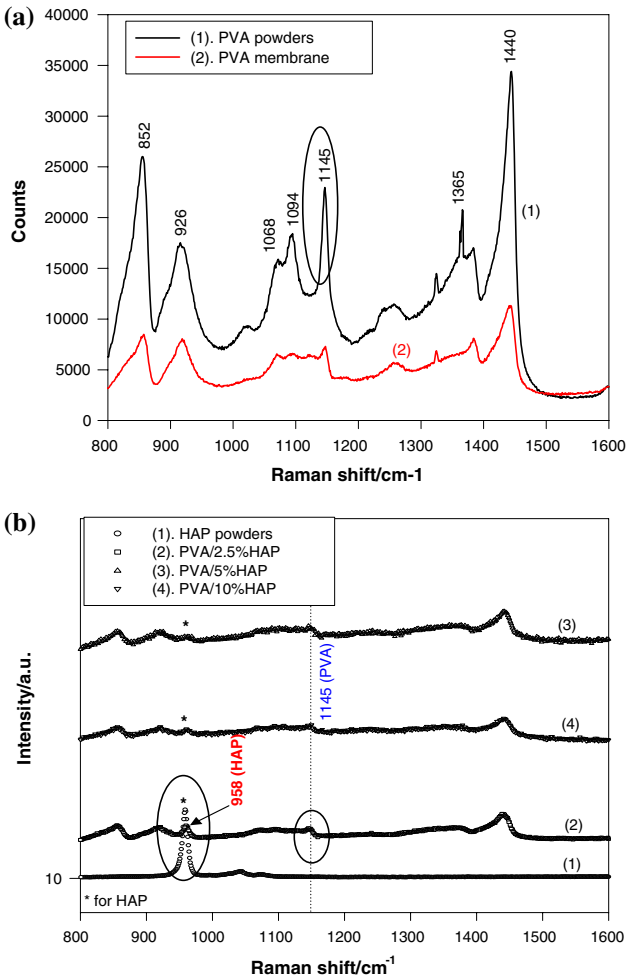

Fig. 4 Micro-Raman spectra for the PVA/HAP composite polymer membranes with different compositions of HAP fillers

Table 2 Assignments for major Raman characteristic peaks of the PVA polymer and HAP filler powders

Frequency (cm^{-1}) PVA polymer	Assignment
852	C–C stretch
926	C–C stretch
1,073	C–O stretch, O–H bend
1,092	C–O stretch, O–H bend
1,145	C–O stretch, C–C stretch
1,360	C–H bend, O–H bend
1,440	C–H bend, O–H bend
HAP powders	
958	$–PO_4$ stretch

vibrational peak at 1,145 cm^{-1} is an indicator for the degree of crystallinity of PVA polymer [24]. On the other hand, some evidence of the decrease of the PVA vibrational peak at 1,145 cm^{-1} has been indeed shown, which has indicated an increase of amorphous domains of the PVA/HAP composite membrane.

3.3 Ionic conductivity measurements

The typical AC impedance spectra of an alkaline PVA/HAP composite polymer membrane by a direct blend of the PVA polymer with 5 wt.% HAP filler at different temperatures are shown in Fig. 5. The AC spectra were typically non-vertical spikes for stainless steel (SS) blocking electrodes, i.e., the SS|PVA/HAP SPE|SS cell. Analysis of the spectra yielded information about the properties of the PVA/HAP polymer electrolyte, such as bulk resistance, R_b. Taking into account the thickness of the composite electrolyte films, the R_b value was converted into the ionic conductivity value, σ, according to the equation: $\sigma = L/R_b \cdot A$, where L is the thickness (cm) of the PVA/HAP polymer membrane, A is the area of the blocking electrode (cm^2), and R_b is the bulk resistance (ohm) of the alkaline composite polymer membrane.

Typically, the R_b values of the PVA/HAP composite polymer membranes are of the order of 1 ohm and are dependent on the contents of HAP fillers and KOH. The composite polymer membrane was immersed in an 8M KOH solution for 24 h before measurement. Table 3 shows the ionic conductivity values of all alkaline PVA/2.5 ~ 10 wt.%HAP composite polymer membranes at different temperatures. As a result, the ionic conductivity value of alkaline PVA/2.5 wt.%HAP composite polymer membranes was 0.0182 S cm^{-1} at 30 °C.

Comparatively, the ionic conductivity values of the alkaline PVA/HAP composite polymer membrane

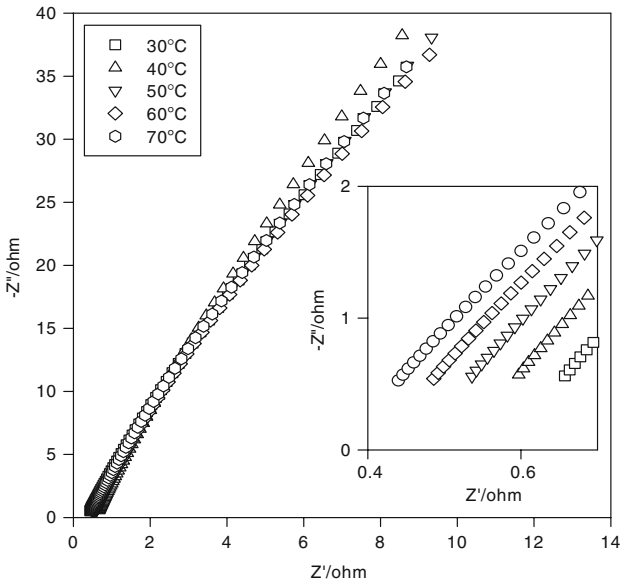

Fig. 5 AC spectra of the PVA/10 wt.%HAP composite polymer membrane in an 8M KOH at different temperatures; the inset for the high frequency area

Table 3 The ionic conductivities of the PVA/HAP composite polymer membranes with different compositions of HAP fillers at different temperatures

σ(S cm^{-1})	PVA composite membranes		
T(°C)	2.5 wt.%HAP	5 wt.%HAP	10 wt.%HAP
30	0.0182	0.0251	0.0442
40	0.0212	0.0272	0.0465
50	0.0263	0.0295	0.0483
60	0.0314	0.0315	0.0514
70	0.0378	0.0335	0.0542

comprising of 5 and 10 wt.% HAP fillers were 0.0251 and 0.0442 S cm^{-1} at 30 °C, respectively. It was found that the highest ionic conductivity value of the alkaline PVA/HAP composite polymer membrane was with 10 wt.% HAP fillers (about 0.0442 S cm^{-1} at ambient temperature). The results indicated that the ionic conductivity of the PVA/HAP composite polymer membranes increased when the content of added HAP ceramic fillers also increased.

3.4 Electrochemical measurements

Figure 6 shows the i–t curves of alkaline DEFC consisting of the PtRu black anode based on the Ni-foam with a loading of PtRu black of 4.0 mg cm^{-2} and an ELAT anode with PtRu/C of 4 mg cm^{-2}, an air cathode with MnO_2/XC-72R carbon inks of 3.63 mg cm^{-2}, a PVA/10 wt.%HAP composite polymer membrane in an 8M KOH + 2M C_2H_5OH solution at 0.40 V, respectively. The mean current densities of the DEFC using lab-made PtRu anode based on the Ni-foam matrix and the E-TEK PtRu anode

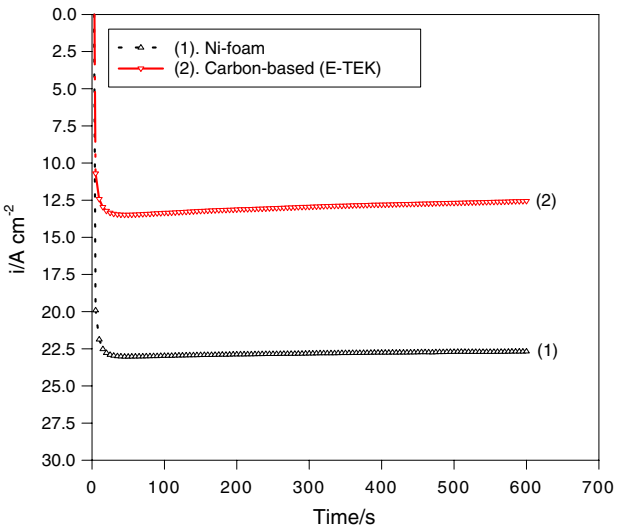

Fig. 6 The chronoamperometries (i–t) curves of the DEFC comprised of the PVA/10%HAP composite polymer membranes in an 8M KOH + 2M ethanol at 0.4 0 V

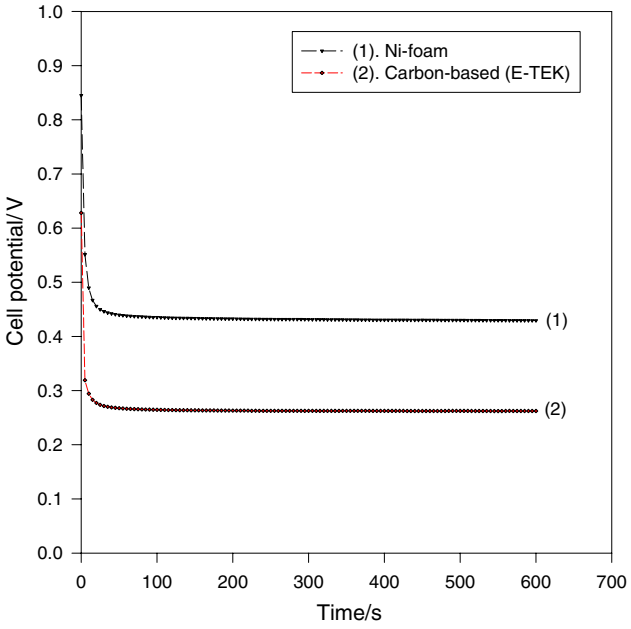

Fig. 7 The E–t curves of the DEFC comprised of PVA/10 wt.%HAP composite polymer membrane in an 8M KOH + 2M ethanol at I = 20 mA cm^{-2}

based on carbon paper are 22.35 and 12.65 mA cm^{-2}, respectively. In spite of a tendency towards a decrease at the beginning of the test, it soon stabilized and remained constant for 10 min. The result revealed improved electrochemical performance of the DEFC using the Ni-foam substrate. In fact, the results indicated that the power density of the DEFC comprising of a lab-made PtRu anode based on Ni-foam in an 8M KOH + 2M C_2H_5OH solution at 0.40 V was approximately 8.94 mW cm^{-2} (0.40 V × 22.35 mA cm^{-2} = 8.94 mW cm^{-2}) at 25 °C and ambient air.

Figure 7 also shows the E–t curves of the alkaline DEFC, comprising the lab-made PtRu anode and an E-TEK PtRu anode, an air cathode, and a PVA/10 wt.%HAP composite polymer membrane in an 8M KOH + 2M C_2H_5OH solution at 20 mA cm^{-2} at 25 °C and ambient air, respectively. The mean potentials of the DEFC with the lab-made PtRu Ni-foam anode and the E-TEK anode were 0.438 and 0.267 V, respectively. In spite of a tendency towards a decrease at the beginning of the test, the cell potentials soon stabilized and remained constant during the test; it showed good electrochemical stability for this alkaline DEFC.

Moreover, Fig. 8 shows the potential-current density and the power density-current density curves of the DEFC comprising different PtRu anodes, i.e., based on Ni-foam and carbon paper, in an 8M KOH + 2M C_2H_5OH solution at 25 °C. Surprisingly, the maximum power density of 10.74 mW cm^{-2} of the alkaline DEFC using a lab-made PtRu anode based on Ni-foam with 4 mg cm^{-2} PtRu black

was achieved at $E_{p,max} = 0.288$ V with a peak current density ($i_{p,max}$) of 37.38 mA cm^{-2}. On the other hand, the maximum power density of the DEFC using an E-TEK PtRu anode with 4 mg cm^{-2} PtRu/C was 7.56 mW cm^{-2} at $E_{p,max} = 0.373$ V with a peak current density of 20.28 mA cm^{-2} at 25 °C. Accordingly, it was clearly demonstrated that the alkaline DEFC showed some advantages using the metallic substrate like the Ni-foam with 85% porosity (which offers more ethanol electro-reaction sites) over the carbon fiber. In particular, the alkaline DEFC comprised an air electrode using non-precious metal catalyst (i.e., with MnO_2/XC-72R catalyst inks instead of with Pt/C inks) and a low-cost composite polymer membrane (i.e., with a cheap non-perfluorosulfonated PVA polymer membrane instead of an expensive Nafion membrane).

It is important to investigate the durability of the PVA/HAP composite membrane on the DEFC under a long-term operation. Figure 9 demonstrates the result of a long-term stability test of the alkaline DEFC at 25 °C and in ambient air. The measurement of the cell potential versus time was recorded at 20 mA cm^{-2} under ambient conditions for 10 h. During the stability test, the measurement was carried out with continuous operation of 2 h and with 10 min rest periods. It was found that the cell working potential of 0.303 V for the alkaline DEFC was stable and flat at 20 mA cm^{-2}. It is also noteworthy that the cell potential returned immediately from 0.303 V back to about 0.775 V (OCP) when the load was off.

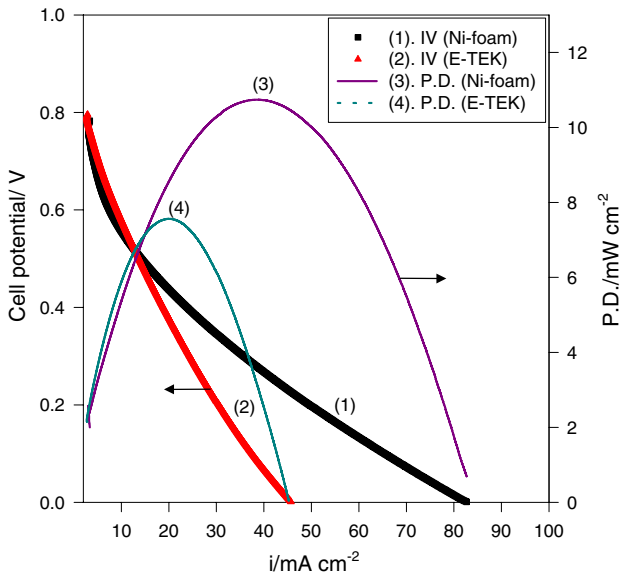

Fig. 8 The I–V and P.D. curves for the DEFC using the PVA/10 wt.%HAP SPE in an 8MKOH + 2M CH_3OH in ambient temperature and pressure

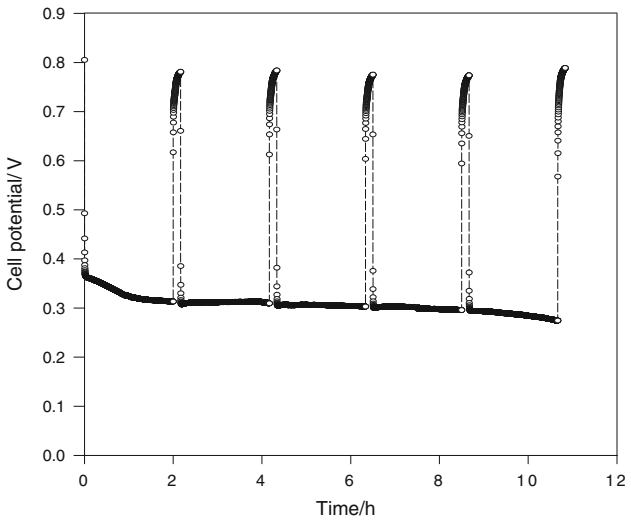

Fig. 9 The long-term stability of the DEFC in an 8M KOH + 2M ethanol at 25 °C

4 Conclusions

The novel composite polymer membrane, based on PVA/HAP, was obtained using a solution casting method. An alkaline direct ethanol fuel cell (DEFC), comprising of the PVA/HAP composite polymer membrane, was assembled and systematically investigated. The DEFC was comprised of an air cathode with MnO_2/XC-72R catalyst inks based on Ni-foam, the lab-made PtRu anode based on the Ni-foam and a PVA/HAP composite polymer membrane. The investigation demonstrated that the alkaline DEFC comprising of a PVA/HAP composite polymer membrane exhibited a good electrochemical performance in ambient temperatures and air. Particularly, the maximum peak power density of the DEFC, using lab-made PtRu anode based on Ni-foam substrate, was 10.74 mW cm^{-2} in ambient temperature and air. From a practical point of view PVA/HAP composite polymer membranes can be prepared through a simple blending process. The PVA/HAP composite polymer membrane is a potential candidate for alkaline DEFC application.

Acknowledgement Financial support from the National Science Council, Taiwan (Project No: NSC-96-2221-E131-032) is gratefully acknowledged.

References

1. Vigier F, Coutanceau C, Hahn F, Belgsir EM, Lamy C (2004) J Electroanal Chem 563:81
2. Spinace EV, Neto AO, Linardi M (2004) J Power Sources 129:121
3. Zhou WL, Song SQ, Li WZ, Sun GQ, Xin Q, Kontou S, Poulianitis K, Tsiakaras P (2004) Solid State Ionics 175:797

4. Liu Z, Ling XY, Su X, Lee JY, Gan LM (2005) J Power Sources 149:1
5. Camara GA, Lima RBD, Iwasita T (2004) Electrochem Commun 6:812
6. Spinace EV, Linardi M, Neto AO (2005) Electrochem Commun 7:365
7. Song SQ, Zhou WJ, Zhou ZH, Jiang LH, Sun GQ, Xin Q, Leontidis V, Kontou S, Tsiakaras P (2005) Int J Hydrogen Energy 30:995
8. Tang X, Zhang B, Li Y, Xu Y, Xin Q, Shen W (2005) J Mol Catal A Chem 235:122
9. Leger JM, Rousseau S, Coutanceau C, Hahn F, Lamy C (2005) Electrochim Acta 50:5118
10. Zhou WJ, Li WZ, Song SQ, Zhou ZH, Jiang LH, Sun GQ, Xin Q, Kontou K, Tsiakaras P (2004) J Power Sources 131:217
11. Tarasevich MR, Karichev ZR, Bogdanovskaya VA, Lubnin EN, Kapustin AV (2005) Electrochem Commun 7:141
12. Bai Y, Wu J, Xi J, Wang J, Zhu W, Chen L, Qiu X (2005) Electrochem Commun 7:1087
13. Xu C, Shen PK, Ji X, Zeng R, Liu Y (2005) Electrochem Commun 7:1305
14. Verma A, Jha AK, Basu S, (2005) ASME J Fuel Cell Sci Technol 2:234
15. Verma A, Jha AK, Basu S (2005) J Power Sources 141:30
16. Verma A, Basu S (2005) J Power Sources 145:282
17. Verma A, Basu S (2007) J Power Sources 168:200
18. Verma A, Basu S (2007) J Power Sources 174:180
19. Yang CC, Lin SJ (2002) J Power Sources 112:497
20. Yang CC (2007) J Membrane Sci 288:51
21. Yang CC, Chiu SJ, Chien WC (2002) J Power Sources 162:21
22. Wang Y, Li L, Hu L, Zhuang L, Lu J, Xu B (2003) Electrochem Commun 5:662
23. Baglio V, Arico AS, Blasi AD, Antonucci V, Antonucci PL, Licoccia S, Traversa E, Fiory FS (2005) Electrochim Acta 50:1241
24. Panero S, Fiorenza P, Navarra MA, Romanowska J, Scrosati B (2005) J Electrochem Soc 152:A2400
25. Park YS, Yamazaki Y (2005) Polymer Bull 53:181